Periocular Recognition under Unconstrained Settings with Universal Background Models

João C. Monteiro and Jaime S. Cardoso
INESC TEC and Faculdade de Engenharia, Universidade do Porto, Porto, Portugal

Keywords: Biometrics, Periocular Recognition, Universal Background Model, SIFT, Gaussian Mixture Models.

Abstract: The rising challenges in the fields of iris and face recognition are leading to a renewed interest in the area. In recent years the focus of research has turned towards alternative traits to aid in the recognition process under less constrained image acquisition conditions. The present work assesses the potential of the periocular region as an alternative to both iris and face in such scenarios. An automatic modeling of SIFT descriptors, regardless of the number of detected keypoints and using a GMM-based Universal Background Model method, is proposed. This framework is based on the Universal Background Model strategy, first proposed for speaker verification, extrapolated into an image-based application. Such approach allows a tight coupling between individual models and a robust likelihood-ratio decision step. The algorithm was tested on the UBIRIS.v2 and the MobBIO databases and presented state-of-the-art performance for a variety of experimental setups.

1 INTRODUCTION

Over the past few years face and iris have been on the spotlight of many research works in biometrics. The *face* is a easily acquirable trait with a high degree of uniqueness, while the *iris*, the coloured part of the eye, presents unique textural patterns resulting from its random morphogenesis during embryonic development (Bakshi et al., 2012). These marked advantages, however, fall short when low-quality images are presented to the system. It has been noted that the performance of iris and face recognition algorithms is severely compromised when dealing with non-ideal scenarios such as non-uniform illumination, pose variations, occlusions, expression changes and radical appearance changes (Bakshi et al., 2012; Boddeti et al., 2011). Several recent works have tried to explore alternative hypothesis to face this problem, either by developing more robust algorithms or by exploring new traits to allow or aid in the recognition process (Woodard et al., 2010).

The *periocular* region is one of such unique traits. Even though a true definition of the periocular region is not standardized, it is common to describe it as the region in the immediate vicinity of the eye (Padole and Proenca, 2012; Smereka and Kumar, 2013). Periocular recognition can be motivated as a middle point between face and iris recognition. It has been shown to present increased performance when only degraded facial data (Miller et al., 2010b) or low quality iris images (Bharadwaj et al., 2010; Tan and Kumar, 2013) are made available, as well as promising results as a soft biometric trait to help improve both face and iris recognition systems in less constrained acquisition environments (Joshi et al., 2012).

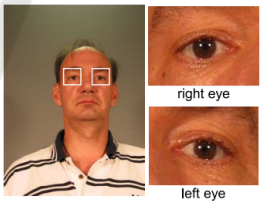

Figure 1: Example of periocular regions from both eyes, extracted from a face image (Woodard et al., 2010).

In this work we present a new approach to periocular recognition under less ideal acquisition conditions. Our proposal is based on the idea of maximum *a posteriori* adaptation of Universal Background Model, as proposed by Reynolds for speaker verification (Reynolds et al., 2000). We evaluate the proposed algorithm on two datasets of color periocular images acquired under visible wavelength (VW) illumination. Multiple noise factors such as varying gazes/poses and heterogeneous lighting conditions are characteristic to such images, thus representing the main challenge of the present work.

The remainder of this paper is organized as fol-

C. Monteiro J. and S. Cardoso J..
Periocular Recognition under Unconstrained Settings with Universal Background Models.
DOI: 10.5220/0005195900380048
In *Proceedings of the International Conference on Bio-inspired Systems and Signal Processing* (BIOSIGNALS-2015), pages 38-48
ISBN: 978-989-758-069-7

lows: Section 2 summarizes relevant works in periocular recognition; Section 3 offers a detailed analysis of the proposed algorithm; Section 4 presents the obtained results and, finally, the main conclusions and future prospects are summarized in Section 5.

2 RELATED WORK

Periocular biometrics is a recent area of research, proposed by the first time in a feasibility study by Park et al. (Park et al., 2009). In this pioneer work, the authors suggested the periocular region as a potential alternative to circumvent the significant challenges posed to iris recognition systems working under unconstrained scenarios. The same authors analysed the effect of degradation on the accuracy of periocular recognition (Park et al., 2011). Performance assessment under less constrained scenarios is also the goal of the work by Miller et al. (Miller et al., 2010a), where factors such as blur and scale are shown to have a severe effect on the performance of periocular recognition. Padole and Proença (Padole and Proenca, 2012) also explore the effect of scale, pigmentation and occlusion, as well as gender, and propose an initial region-of-interest detection step to improve recognition accuracy.

Ross et al. (Ross et al., 2012) explored information fusion based on several feature extraction techniques, to handle the significant variability of input periocular images. Information fusion has become one of the trends in biometric research in recent years and periocular recognition is no exception. Bharadwaj et al. (Bharadwaj et al., 2010) proposed fusion of matching scores from both eyes to improve the individual performance of each of them. On the other hand, Woodard et al. (Woodard et al., 2010) place fusion at the feature level, using color and texture information.

Some works have explored the advantages of the periocular region as an aid to more traditional approaches based on iris. Boddeti et al. (Boddeti et al., 2011) propose the score level fusion of a traditional iris recognition algorithm, based on Gabor features, and a periocular probabilistic approach based on optimal trade-off synthetic discriminant functions (OTSDF). A similar work by Joshi et al. (Joshi et al., 2012) proposed feature level fusion of wavelet coefficients and LBP features, from the iris and periocular regions respectively, with considerable performance improvement over both singular traits. A recent work by Tan et al. (Tan and Kumar, 2013) has also explored the benefits of periocular recognition when highly degraded regions result from the traditional iris segmentation step. The authors have observed discouraging performance when the iris region alone is considered in such scenarios, whereas introducing information from the whole periocular region lead to a significant improvement.

Two other recent and relevant works by Moreno et al. (Moreno et al., 2013b; Moreno et al., 2013a) explore the well-known approach of sparse representation classification in the scope of the specific problem of periocular recognition. A thorough review of the most relevant method in recent years concerning periocular recognition and its main advantages can be found in the work by Santos and Proença (Santos and Proença, 2013).

On the present work we propose a new approach to periocular recognition, based on a general framework with proven results in voice biometrics. We explore a strategy based on the adaptation of a Universal Background Model (UBM) to achieve faster and more robust training of individual specific models. With such idea in mind we aim not only to design a high performance recognition system but also to assess the versatility and robustness of the UBM strategy for biometric traits other than voice.

3 PROPOSED METHODOLOGY

3.1 Algorithm Overview

The proposed algorithm is schematically represented in Figure 2. The two main blocks - *enrollment* and *recognition* - refer to the typical architecture of a biometric system. During enrollment a new individual's biometric data is inserted into a previously existent database of individuals. Such database is probed during the recognition process to assess either the validity of an identity claim - *verification* - or the k most probable identities - *identification* - given an unknown sample of biometric data.

During the enrollment, a set of N models describing the unique statistical distribution of biometric features for each individual $n \in \{1,\ldots,N\}$ is trained by maximum *a posteriori* (MAP) adaptation of an Universal Background Model (UBM). The UBM is a representation of the variability that the chosen biometric trait presents in the universe of all individuals. MAP adaptation works as a specialization of the UBM based on each individual's biometric data. The idea of MAP adaptation of the UBM was first proposed by Reynolds (Reynolds et al., 2000), for speaker verification, and will be further motivated in the following sections.

The recognition phase is carried out through the

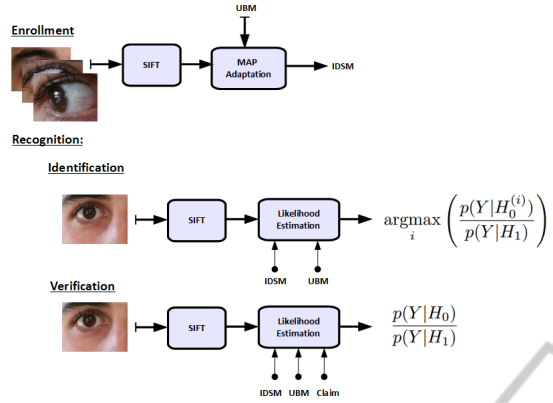

Figure 2: Graphical representation of the main steps in both the enrollment and recognition (verification and identification) phases of the proposed periocular recognition algorithm.

projection of the features extracted from an unknown sample onto both the UBM and the individual specific models (IDSM) of interest. A likelihood-ratio between both projections outputs the final recognition score. Depending on the functioning mode of the system - verification or identification - decision is carried out by thresholding or maximum likelihood-ratio respectively.

3.2 Universal Background Model

Universal background modeling is a common strategy in the field of voice biometrics (Povey et al., 2008). It can be easily understood if the problem of biometric verification is interpreted as a basic hypothesis test. Given a biometric sample Y and a claimed ID, S, we define:

$$H_0\text{: } Y \text{ belongs to } S$$
$$H_1\text{: } Y \text{ does not belong to } S$$

as the null and alternative hypothesis, respectively. The optimal decision is taken by a *likelihood-ratio test*:

$$\frac{p(Y|H_0)}{p(Y|H_1)} \begin{cases} \geq \theta & \text{accept } H_0 \\ \leq \theta & \text{accept } H_1 \end{cases} \quad (1)$$

where θ is the decision threshold for accepting or rejecting H_0, and $p(Y|H_i), i \in \{0,1\}$ is the likelihood of observing sample Y when we consider hypothesis i to be true.

Biometric recognition can, thus, be reduced to the problem of computing the likelihood values $p(Y|H_0)$ and $p(Y|H_1)$. It is intuitive to note that H_0 should be represented by a model λ_{hyp} that characterizes the hypothesized individual, while, alternatively, the representation of H_1, $\lambda_{\overline{hyp}}$, should be able to model *all the alternatives to the hypothesized individual*.

From such formulation arises the need for a model that successfully covers the space of alternatives to the hypothesized identity. The most common designation in literature for such a model is *universal background model* or *UBM* (Reynolds, 2002). Such model must be trained on a large set of data, so as to faithfully cover a representative user space and a significant amount of sources of variability. The following section details the chosen strategy to model $\lambda_{\overline{hyp}}$ and how individual models, λ_{hyp}, can be adapted from the UBM in a fast and robust way.

3.3 Hypothesis Modeling

On the present work we chose Gaussian Mixture Models (GMM) to model both the UBM, i.e. $\lambda_{\overline{hyp}}$, and the individual specific models (IDSM), i.e. λ_{hyp}. Such models are capable of capturing the empirical probability density function (PDF) of a given set of feature vectors, so as to faithfully model their intrinsic statistical properties (Reynolds et al., 2000). The choice of GMM to model feature distributions in biometric data is extensively motivated in many works of related areas. From the most common interpretations, GMMs are seen as capable of representing broad "hidden" classes, reflective of the unique structural arrangements observed in the analysed biometric traits (Reynolds et al., 2000). Besides this assumption, Gaussian mixtures display both the robustness of parametric unimodal Gaussian density estimates, as well as the ability of non-parametric models to fit non-Gaussian data (Reynolds, 2008). This duality, alongside the fact that GMM have the noteworthy strength of generating smooth parametric densities, confers such models a strong advantage as generative model of choice. For computational efficiency, GMM models are often trained using diagonal covariance matrices. This approximation is often found in biometrics literature, with no significant accuracy loss associated (Xiong et al., 2006).

All models are trained on sets of Scale Invariant Feature Transform (SIFT) keypoint descriptors (Lowe, 2004). This choice for periocular image description is thoroughly motivated in literature (Ross et al., 2012; Park et al., 2011), mainly due to the observation that local descriptors work better than their global counterparts when the available data presents non-uniform conditions. Furthermore, the invariance of SIFT features to a set of common undesirable factors (image scaling, translation, rotation and also partially to illumination and affine or $3D$ projection), confer them a strong appeal in the area of uncon-

strained biometrics.

Originally such descriptors are defined in 128 dimensions. However, we chose to perform a Principle Component Analysis (PCA), as suggested in (Shinoda and Inoue, 2013), reducing the dimensionality to 32. Such reduction allows not only a significant reduction in the computational complexity of the training phase, but also an improved distinctiveness and robustness to the extracted feature vectors, especially as far as image deformation is concerned (Ke and Sukthankar, 2004). We computed the principle components from the same data used to train the UBM.

3.4 H_1: UBM Parameter Estimation

To train the Universal Background Model a large amount of "impostor" data, i.e. a set composed of data from all the enrolled individuals, is used, so as to cover a wide range of possibilities in the individual search space (Shinoda and Inoue, 2013). The training process of the UBM is simply performed by fitting a k-mixture GMM to the set of PCA-reduced feature vectors extracted from all the "impostors".

If we interpret the UBM as an "impostor" model, its "genuine" counterpart can be obtained by adaptation of the UBM's parameters, $\lambda_{\overline{hyp}}$, using individual specific data. For each enrolled individual, *ID*, an *individual specific model* (IDSM), defined by parameters λ_{hyp}, is therefore obtained. The adaptation process will be outlined in the following section.

3.5 H_0: MAP Adaptation of the UBM

IDSMs are generated by the *tuning of the UBM parameters* in a maximum *a posteriori* (MAP) sense, using individual specific biometric data. This approach provides a tight coupling between the IDSM and the UBM, resulting in better performance and faster scoring than uncoupled methods (Xiong et al., 2006), as well as a robust and precise parameter estimation, even when only a small amount of data is available (Shinoda and Inoue, 2013). This is indeed one of the main advantages of using UBMs. The determination of appropriate initial values (i.e. seeding) of the parameters of a GMM remains a challenging issue. A poor initialization may result in a weak model, especially when the data volume is small. Since the IDSM are learnt only from each individual data, they are more prone to a poor convergence that the GMM for the UBM, learnt from a big pool of individuals. In essence, UBM constitutes a good initialization for the IDSM.

The adaptation process, as proposed by Reynolds (Reynolds et al., 2000), resembles the Expectation-Maximization (EM) algorithm, with two main estimation steps. The first is similar to the expectation step of the EM algorithm, where, for each mixture of the UBM, a set of sufficient statistics are computed from a set of M individual specific feature vectors, $X = \{\mathbf{x}_1 ... \mathbf{x}_M\}$:

$$n_i = \sum_{m=1}^{M} p(i|\mathbf{x}_m) \tag{2}$$

$$E_i(\mathbf{x}) = \frac{1}{n_i} \sum_{m=1}^{M} p(i|\mathbf{x}_m)\mathbf{x}_m \tag{3}$$

$$E_i(\mathbf{x}\mathbf{x}^t) = \frac{1}{n_i} \sum_{m=1}^{M} p(i|\mathbf{x}_m)\mathbf{x}_m\mathbf{x}_m^t \tag{4}$$

where $p(i|\mathbf{x}_m)$ represents the probabilistic alignment of $\mathbf{x}_m$ into each UBM mixture. Each UBM mixture is then adapted using the newly computed sufficient statistics, and considering diagonal covariance matrices. The update process can be formally expressed as:

$$\hat{w}_i = [\alpha_i n_i/M + (1-\alpha_i)w_i]\xi \tag{5}$$

$$\hat{\mu}_i = \alpha_i E_i(\mathbf{x}) + (1-\alpha_i)\mu_i \tag{6}$$

$$\hat{\Sigma}_i = \alpha_i E_i(\mathbf{x}\mathbf{x}^t) + (1-\alpha_i)(\sigma_i\sigma_i^t + \mu_i\mu_i^t) - \hat{\mu}_i\hat{\mu}_i^t \tag{7}$$

$$\sigma_i = \mathrm{diag}(\Sigma_i) \tag{8}$$

where $\{w_i, \mu_i, \sigma_i\}$ are the original UBM parameters and $\{\hat{w}_i, \hat{\mu}_i, \hat{\sigma}_i\}$ represent their adaptation to a specific speaker. To assure that $\sum_i w_i = 1$ a weighting parameter ξ is introduced. The α parameter is a data-dependent adaptation coefficient. Formally it can be defined as:

$$\alpha_i = \frac{n_i}{r + n_i} \tag{9}$$

where r is generally known as the *relevance factor*. The individual dependent adaptation parameter serves the purpose of weighting the relative importance of the original values and the new sufficient statistics in the adaptation process. For the UBM adaptation we set $r = 16$, as this is the most commonly observed value in literature (Reynolds et al., 2000). Most works propose the sole adaptation of the mean values, i.e. $\alpha_i = 0$ when computing $\hat{w}_i$ and $\hat{\sigma}_i$. This simplification seems to bring no nefarious effects over the performance of the recognition process, while allowing faster training of the individual specific models (Kinnunen et al., 2009).

3.6 Recognition and Decision

After the training step of both the UBM and each IDSM, the recognition phase with new data from an unknown source is somewhat trivial. As referred in previous sections, the identity check is performed through the projection of the new test data, $X_{test} = \{\mathbf{x}_{t,1}, \ldots, \mathbf{x}_{t,N}\}$, where $\mathbf{x}_{t,i}$ is the i-th PCA-reduced SIFT vector extracted from the periocular region of test subject t, onto both the UBM and either the claimed IDSM (in verification mode) or all such models (in identification mode). The recognition score is obtained as the average likelihood-ratio of all keypoint descriptors $\mathbf{x}_{t,i}, \forall i \in \{1..N\}$. The decision is then carried out by checking the condition presented in Equation (1), in the case of verification, or by detecting the maximum likelihood-ratio value for all enrolled IDs, in the case of identification.

This is a second big advantage of using UBM. The ratio between the IDSM and the UBM probabilities of the observed data is a more robust decision criterion than relying solely on the IDSM probability. This results from the fact that some subjects are more prone to generate high likelihood values than others, i.e. some people have a more "generic" look than others. The use of a likelihood ratio with an universal reference works as a normalization step, mapping the likelihood values in accord to their global projection. Without such step, finding a global optimal value for the decision threshold, θ, presented in Equation 1 would be a far more complex process.

4 EXPERIMENTAL RESULTS

In this section we start by presenting the datasets and the experimental setups under which performance was assessed. Further sections present a detailed analysis regarding the effect of model complexity and fusion of color channels in the global performance of the proposed algorithm.

4.1 Tested Datasets

The proposed algorithm was tested on two noisy color iris image databases: UBIRIS.v2 and MobBIO. Even though both databases were designed in an attempt to promote the development of robust iris recognition algorithms for images acquired under VW illumination, their intrinsic properties make them attractive to study the feasibility of periocular recognition under similar conditions. The following sections detail their main features as well as the reasoning behind their choice.

4.1.1 UBIRIS.v2 Database

Images in UBIRIS.v2 (Proença et al., 2010) database were captured under non-constrained conditions (at-a-distance, on-the-move and on the visible wavelength), with corresponding realistic noise factors. Figure 3 depicts some examples of these noise factors (reflections, occlusions, pigmentation, etc.). Two acquisition sessions were performed with 261 individuals involved and a total of 11100 300×400 color images acquired. Each individual's images were acquired at variable distances with 15 images per eye and per season. Even though the UBIRIS.v2 database was primarily developed to allow the study of unconstrained iris recognition, many works have explored its potential for periocular-based strategies as an alternative to low-quality iris recognition (Bharadwaj et al., 2010; Joshi et al., 2012; Padole and Proenca, 2012).

(a) (b) (c) (d)

Figure 3: Examples of noisy image from the UBIRIS.v2 database.

4.1.2 MobBIO Database

The MobBIO multimodal database (Sequeira et al., 2014) was created in the scope of the 1st Biometric Recognition with Portable Devices Competition 2013, integrated in the ICIAR 2013 conference. The main goal of the competition was to compare various methodologies for biometric recognition using data acquired with portable devices. We tested our algorithm on the iris modality present on this database. Regarding this modality the images were captured under two alternative lighting conditions, with variable eye orientations and occlusion levels, so as to comprise a larger variability of unconstrained scenarios. Distance to the camera was, however, kept constant for each individual. For each of the 105 volunteers 16 images (8 of each eye) were acquired. These images were obtained by cropping a single image comprising both eyes. Each cropped image was set to a 300×200 resolution. Figure 4 depicts some examples of such images.

The MobBIO database presents a face modality which has also been explored for comparative purposes in the present work. Images were acquired in similar conditions to those described above for iris images, with 16 images per subject. Examples of such images can be observed in Figure 5.

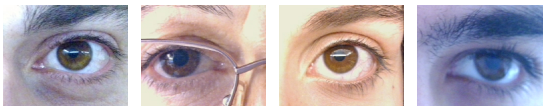

(a) (b) (c) (d)

Figure 4: Examples of iris images in the MobBIO database.

(a) (b) (c) (d)

Figure 5: Examples of face images in the MobBIO database.

4.2 Evaluation Metrics

Performance was evaluated for both verification and identification modes. Regarding the former we analyzed the *equal error rate* (EER) and the *decidability index* (DI). The EER is observed at the decision threshold, θ, where the errors of falsely accepting and falsely rejecting H_0 occur with equal frequency. The global behavior of both types of errors is often analyzed through receiver operating characteristic (ROC) curves. On the other hand, the DI quantifies the separation of the "genuine" and "impostor" likelihood score distributions, as follows:

$$DI = \frac{|\mu_g - \mu_i|}{\sqrt{0.5(\sigma_g^2 + \sigma_i^2)}} \tag{10}$$

where (μ_g, σ_g) and (μ_i, σ_i) are the mean and standard deviation of the genuine and impostor score distributions, respectively.

For identification we analyze cumulative match curves (CMC). These curves represent the rate of correctly identified individuals, by checking if the true identity is present in the N highest ranked identities. The N parameter is generally referred to as rank. That allows us to define the *rank-1 recognition rate* as the value of the CMC at $N = 1$.

4.3 Experimental Setups

Our experiments were conducted in three distinct experimental setups, two of them regarding the UBIRIS.v2 database and the remaining one the MobBIO database:

1. In the first setup, for the UBIRIS.v2 images, six samples from 80 different subjects were used, captured from different distances (4 to 8 meters), with varying gazes/poses and notable changes in lighting conditions. One image per individual was randomly chosen as probe, whereas the remaining five samples were used for the UBM training and MAP adaptation. The results were cross-validated by changing the probe image, per subject, for each of the six chosen images.
2. Many works on periocular biometrics evaluate their results using a well-known subset of the UBIRIS.v2 database, used in the context of the NICE II competition (Proença, 2009). This dataset is divided in train and test subsets, with a total of 1000 images from 171 individuals. In the present work we choose to use test subset, composed by 904 images from 152 individuals. Only individuals with more than 4 available images were considered, as 4 images were randomly chosen for training and the rest for testing. Results were cross-validated 10-fold. The train dataset composed by the remaining 96 images from 19 individuals was employed in the parameter optimization step described in further sections.
3. Concerning the MobBIO database, 8 images were randomly chosen from each of the 105 individuals for the training of the models, whereas the remaining 8 were chosen for testing. The process was cross-validated 10-fold. For comparative purposes a similar experiment was carried out on face images from the same 105 individuals, using the same $8+8$ image distribution.

As both databases are composed by color images, each of the RGB channels was considered individually for the entire enrollment and identification process. For the parameter optimization described in the next section images were previously converted to grayscale.

4.4 Parameter Optimization

A smaller dataset, for each database, was also designed to optimize the the number of GMM mixtures of the trained models. For the UBIRIS.v2 we chose to work with the well-known train dataset from the NICE II competition (Proença, 2009), composed by 96 images from 19 individuals. For the MobBIO database we chose a total of 50 images from 10 individuals to perform the previously referred optimization. The obtained performance was cross-validated using a leave-one-out strategy. The chosen metric to evaluate performance was the rank-1 recognition rate (R_1). The evolution of performance with the optimization parameter can be observed in Figure 6. With such results in mind, the recognition performance for the experimental setups presented in the last section was assessed for a number of mixtures $M = 128$ and

$M = 64$ for the UBIRIS.v2 and MobBIO databases respectively. We choose both these values as the values where a performance plateau is achieved in the graph of Figure 6. We chose the lowest possible values for the parameter M so as to minimize the computational complexity of the UBM training, which constitutes the limiting step of the process, without a significant loss in performance.

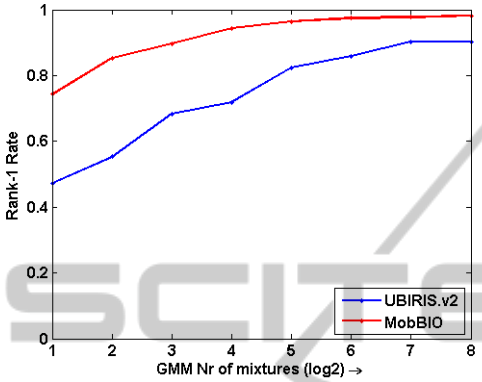

Figure 6: Recognition rates obtained with the optimization subset for variable values of parameter M, number of mixtures in the trained GMMs.

4.5 Recognition Results

The results obtained for both databases and experimental setups are represented through ROC and CMC curves on Figures 7(a) to 7(f). A comparison with some state-of-the-art algorithms in the UBIRIS.v2 database is also presented in Table 1. In this table results are grouped according to the experimental setup of each reported work and also the studied trait: P - Periocular, I - Iris or $P+I$ - Fusion of both traits.

Besides testing each of the RGB channels individually, a simple sum-rule score-level fusion strategy (Kittler et al., 1998) was also considered. It is easily discernible, from the observation of Figure 7, that the fusion of information from multiple color channels brings about a significant improvement in performance for all the tested datasets. When comparing the results obtained with this approach with some state-of-the-art algorithms a few points deserve further discussion. First, the proposed algorithm is capable of achieving and even surpassing state-of-the-art performance in multiple experimental setups. Concerning the most common of such setups (2), it is interesting to note that a few works attempted to explore the UBIRIS.v2 dataset for iris recognition. The obtained performance has been considered "discouraging" in the work by Kumar et al. (Kumar and Chan, 2012). Comparing the rank-1 recognition rate obtained with our algorithm (88.93%) with the 48.1% reported in the former work, we conclude that the periocular region may represent a viable alternative to iris in images acquired under visible wavelength (VW) illumination. Such acquisition conditions are known to increase light reflections from the cornea, resulting in a sub-optimal signal-to-noise ratio (SNR) in the sensor, lowering the contrast of iris images and the robustness of the system (Proença, 2011). More recent works have explored multimodal approaches, using combined information from both the iris and the periocular region. Analysis of Table 1 shows that none of such works reaches the performance reported in the present work for the same experimental setup. Such observation might indicate that most discriminative biometric information from the UBIRIS.v2 images might be present in the periocular region, and that considering data from the very noisy iris regions might only result in a degradation of the performance obtained by the periocular region alone.

Concerning the MobBIO database, an alternative comparison was carried out to analyze the potential of the periocular region as an alternative to face recognition. The observed performance for periocular images was considerably close to that using full-face information, with rank-1 recognition rates of 98.98% and 99.77% respectively. These results are an indication that, under more ideal acquisition conditions, there is enough discriminative potential in the periocular region alone to rival with the full face in terms of recognition performance. In scenarios where some parts of the face are purposely disguised (scarves covering the mouth for example) this observation might indicate that a non-corrupted periocular region can, indeed, overperform recognition with the occluded full-face images. Such conditions were not tested in the present work but might be the basis for an interesting follow-up. Even though the observed results are promising, it must be noted that the noise factors present in the MobBIO database are still far from a highly unconstrained scenario.

The robustness of the likelihood-ratio decision step was also assessed. We compared the performance observed for the scores obtained with Equation 1 and the scores obtained using only its numerator, i.e. only the likelihood of each test image without the UBM normalization. For the experimental setup (2) we obtained an average rank-1 recognition rate of 43.6%, whereas the MobBIO experimental setup (3) resulted in 90.5% for the same metric. It is easily noted that performance is less compromised in the MobBIO database. Considering only the numerator of Equation 1 is the same as considering a constant denominator value for every tested image. As the denominator represents the projection of the tested im-

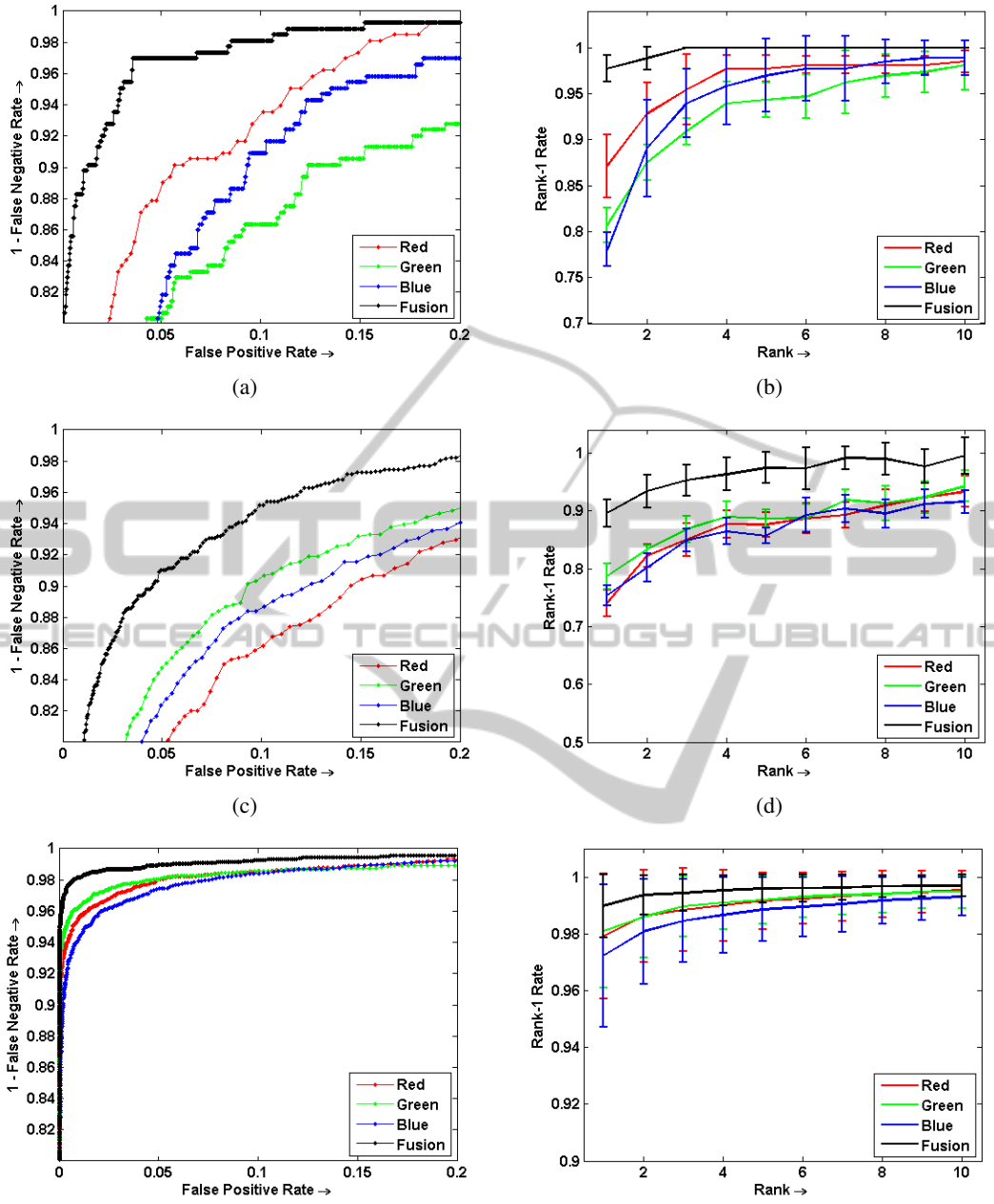

Figure 7: ROC and CMC curves for: (a-b) UBIRIS.v2 database, setup (1); (c-d) UBIRIS.v2 database, setup (2) and (e-f) MobBIO database, setup (3);. ROC curves present the average results of cross-validation, whereas CMCs present the average value and error-bars for the first 10 ranked IDs in each setup.

ages on the UBM, this alternative decision strategy might be interpreted as assuming a constant background for every tested image. From the observed results we might conclude that such assumption fits better the images from the MobBIO database. We also note that for more challenging scenarios, where the constant background assumption fails, the use of background normalization produces a significant improvement in performance.

A few last considerations regarding the discriminative potential of the proposed algorithm may be taken from the observation of Figure 8. On each row we analyze the 4 highest ranked models for the images presented in the first column. The first two

Table 1: Comparison between the average obtained results with both experimental setups for the UBIRIS.v2 database and some state-of-the-art algorithms.

Work	*Setup*	*Traits*	R_1	*EER*	D_i
Proposed	1	*P*	**97.73%**	**0.0452**	4.9795
Proposed	2	*P*	**88.93%**	**0.0716**	**3.6141**
Moreno et al. (Moreno et al., 2013a)	1	*P*	97.63%	0.1417	–
Tan et al. (Tan and Kumar, 2013)	2	*P*+*I*	39.4%	–	–
Tan et al. (Tan et al., 2011)	2	*P*+*I*	–	–	2.5748
Kumar et al. (Kumar and Chan, 2012)	2	*I*	48.01%	–	–
Proença et al. (Proença and Santos, 2012)	2	*I*	–	≈ 0.11	2.848

rows depict correct identifications. It is interesting to note how each of the 4 highest ranked identities in the second row correspond to individuals wearing glasses. Such observation seems to indicate that the proposed modeling process is capable of describing high-level global features, such as glasses. Furthermore, the fact that the correct ID was guessed also demonstrates its capacity of distinguishing between finer details separating individual models. The third and fourth rows present some test images whose ID was not correctly assessed by the algorithm. In the third row we present a case where even though the correct ID and the most likely model were not correctly paired, the correct guess still appears in the top ranked models. We note that even a human user analyzing the four highest ranked models would find it very difficult to detect significant differences. The fourth row presents the extreme case where none of the top ranked models correspond to the true ID. It is worth noting how the test images presented in the third and fourth rows are very similar to a large number of images present in other individual's models. This observation leads to the hypothesis that *some users are easier to identify than others inside a given population*, an effect known as the *Doddington zoo effect* (Ross et al., 2009). It also shows that the proposed algorithm is capable of narrowing the range of possible identities to those subjects who "look more alike".

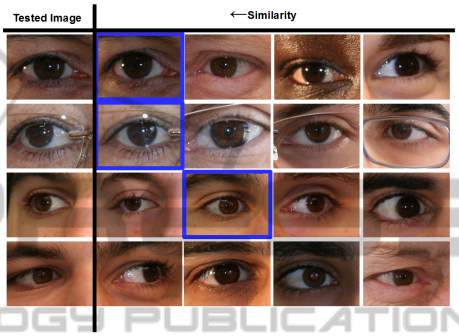

Figure 8: Identification results for rank-4 in the UBIRIS.v2 database. The first column depicts the tested images while the remaining 4 images exemplify representative images from the 4 most probable models, after the recognition is performed. The blue squares mark the true identity.

4.6 Implementation Details

The proposed algorithm was developed in MATLAB R2012a and tested on a PC with 3.40GHz Intel(R) Core(TM) i7-2600 processor and 8GB RAM. To train the GMM's we used the Netlab toolbox (Nabney, 2004), whereas SIFT keypoint extraction and description was performed using the VLFeat toolbox (Vedaldi and Fulkerson, 2010). For a single identity check, using the UBIRIS.v2 database and $M = 128$, we observed a processing time of $0.0586 \pm 0.0088s$.

5 CONCLUSIONS AND FUTURE WORK

In the present work we propose an automatic modeling of SIFT descriptors, using a GMM-based UBM method, to achieve a canonical representation of individual's biometric data, regardless of the number of detected SIFT keypoints. We tested the proposed algorithm on periocular images from two databases and achieved state-of-the-art performance for all experimental setups. Periocular recognition has been the focus of many recent works that explore it as a viable alternative to both iris and face recognition under less ideal acquisition scenarios.

Even though we propose the algorithm for periocular recognition, the framework can be easily extrapolated for other image-based traits. To the extent of our knowledge, GMM-based UBM methodologies were solely explored for speaker recognition so far. The proposed work may, thus, represent the first of a series of experiments that explore its main advantages in the scope of multiple trending biometric topics. For example, the fact that any number of keypoints triggers a recognition score may be relevant when only

partial or occluded data is available for recognition. Scenarios, like the one described in the last section, where faces are purposely occluded may be an interesting area to explore.

Besides from the conceptual advantages of the proposed algorithm, a few technical details may be improved in further works. Exploring further color channels besides the RGB space could bring benefits to the proposed algorithm. Regarding fusion, exploring individual specific parameters instead of a global parametrization, would enable the algorithm to be trained to counter the Doddington zoo effect. As not all people are as easy to identify, fitting the properties of the designed classification block to adapt to different classes of individuals seems like an interesting idea.

Finally, and regarding the training setup, some questions might be worthy of a more thorough research. In the case of voice recognition it is common to train two separate UBMs for male and female speakers. Extrapolating this idea to image-based traits, multiple UBMs trained on homogeneous sets of equally or similarly zoomed images might improve the results when more realistic and dynamic conditions are presented to the acquisition system. In a related topic it is also not consensual whether the left and right eyes, due to the intrinsic symmetry of the face, should be considered in a single model or as separate entities. All the aforementioned questions demonstrate how much the present results can be improved, leaving some promising prospects for future works.

REFERENCES

Bakshi, S., Kumari, S., Raman, R., and Sa, P. K. (2012). Evaluation of periocular over face biometric: A case study. *Procedia Engineering*, 38:1628–1633.

Bharadwaj, S., Bhatt, H. S., Vatsa, M., and Singh, R. (2010). Periocular biometrics: When iris recognition fails. In *4th IEEE International Conference on Biometrics: Theory Applications and Systems*, pages 1–6.

Boddeti, V. N., Smereka, J. M., and Kumar, B. V. (2011). A comparative evaluation of iris and ocular recognition methods on challenging ocular images. In *2011 International Joint Conference on Biometrics*, pages 1–8. IEEE.

Joshi, A., Gangwar, A. K., and Saquib, Z. (2012). Person recognition based on fusion of iris and periocular biometrics. In *Hybrid Intelligent Systems (HIS), 2012 12th International Conference on*, pages 57–62. IEEE.

Ke, Y. and Sukthankar, R. (2004). Pca-sift: A more distinctive representation for local image descriptors. In *Computer Vision and Pattern Recognition, 2004. CVPR 2004. Proceedings of the 2004 IEEE Computer Society Conference on*, volume 2, pages II–506. IEEE.

Kinnunen, T., Saastamoinen, J., Hautamaki, V., Vinni, M., and Franti, P. (2009). Comparing maximum a posteriori vector quantization and gaussian mixture models in speaker verification. In *IEEE International Conference on Acoustics, Speech and Signal Processing*, pages 4229–4232. IEEE.

Kittler, J., Hatef, M., Duin, R. P., and Matas, J. (1998). On combining classifiers. *Pattern Analysis and Machine Intelligence, IEEE Transactions on*, 20(3):226–239.

Kumar, A. and Chan, T.-S. (2012). Iris recognition using quaternionic sparse orientation code (qsoc). In *2012 IEEE Computer Society Conference on Computer Vision and Pattern Recognition Workshops*, pages 59–64.

Lowe, D. G. (2004). Distinctive image features from scale-invariant keypoints. *International journal of computer vision*, 60(2):91–110.

Miller, P. E., Lyle, J. R., Pundlik, S. J., and Woodard, D. L. (2010a). Performance evaluation of local appearance based periocular recognition. In *IEEE International Conference on Biometrics: Theory, Applications, and Systems*, pages 1–6.

Miller, P. E., Rawls, A. W., Pundlik, S. J., and Woodard, D. L. (2010b). Personal identification using periocular skin texture. In *2010 ACM Symposium on Applied Computing*, pages 1496–1500. ACM.

Moreno, J. C., Prasath, V., and Proença, H. (2013a). Robust periocular recognition by fusing local to holistic sparse representations. In *Proceedings of the 6th International Conference on Security of Information and Networks*, pages 160–164. ACM.

Moreno, J. C., Prasath, V. B. S., Santos, G. M. M., and Proença, H. (2013b). Robust periocular recognition by fusing sparse representations of color and geometry information. *CoRR*, abs/1309.2752.

Nabney, I. T. (2004). *NETLAB: algorithms for pattern recognition*. Springer.

Padole, C. N. and Proenca, H. (2012). Periocular recognition: Analysis of performance degradation factors. In *5th IAPR International Conference on Biometrics*, pages 439–445.

Park, U., Jillela, R. R., Ross, A., and Jain, A. K. (2011). Periocular biometrics in the visible spectrum. *IEEE Transactions on Information Forensics and Security*, 6(1):96–106.

Park, U., Ross, A., and Jain, A. K. (2009). Periocular biometrics in the visible spectrum: A feasibility study. In *IEEE 3rd International Conference on Biometrics: Theory, Applications, and Systems*, pages 1–6.

Povey, D., Chu, S. M., and Varadarajan, B. (2008). Universal background model based speech recognition. In *IEEE International Conference on Acoustics, Speech and Signal Processing*, pages 4561–4564.

Proença, H. (2009). NICE:II: Noisy iris challenge evaluation - part ii. http://http://nice2.di.ubi.pt/.

Proença, H. (2011). Non-cooperative iris recognition: Issues and trends. In *19th European Signal Processing Conference*, pages 1–5.

Proença, H. and Santos, G. (2012). Fusing color and shape descriptors in the recognition of degraded iris images acquired at visible wavelengths. *Computer Vision and Image Understanding*, 116(2):167–178.

Proença, H., Filipe, S., Santos, R., Oliveira, J., and Alexandre, L. A. (2010). The ubiris.v2: A database of visible wavelength iris images captured on-the-move and at-a-distance. *IEEE Transactions on Pattern Analysis and Machine Intelligence*, 32(8):1529–1535.

Reynolds, D. (2008). Gaussian mixture models. *Encyclopedia of Biometric Recognition*, pages 12–17.

Reynolds, D., Quatieri, T., and Dunn, R. (2000). Speaker verification using adapted gaussian mixture models. *Digital signal processing*, 10(1):19–41.

Reynolds, D. A. (2002). An overview of automatic speaker recognition technology. In *Acoustics, Speech, and Signal Processing (ICASSP), 2002 IEEE International Conference on*, volume 4, pages IV–4072. IEEE.

Ross, A., Jillela, R., Smereka, J. M., Boddeti, V. N., Kumar, B. V., Barnard, R., Hu, X., Pauca, P., and Plemmons, R. (2012). Matching highly non-ideal ocular images: An information fusion approach. In *Biometrics (ICB), 2012 5th IAPR International Conference on*, pages 446–453. IEEE.

Ross, A., Rattani, A., and Tistarelli, M. (2009). Exploiting the doddington zoo effect in biometric fusion. In *Biometrics: Theory, Applications, and Systems, 2009. BTAS'09. IEEE 3rd International Conference on*, pages 1–7. IEEE.

Santos, G. and Proença, H. (2013). Periocular biometrics: An emerging technology for unconstrained scenarios. In *Computational Intelligence in Biometrics and Identity Management (CIBIM), 2013 IEEE Workshop on*, pages 14–21. IEEE.

Sequeira, A. F., Monteiro, J. C., Rebelo, A., and Oliveira, H. P. (2014). MobBIO: a multimodal database captured with a portable handheld device. In *Proceedings of International Conference on Computer Vision Theory and Applications (VISAPP)*.

Shinoda, K. and Inoue, N. (2013). Reusing speech techniques for video semantic indexing [applications corner]. *Signal Processing Magazine, IEEE*, 30(2):118–122.

Smereka, J. M. and Kumar, B. (2013). What is a" good" periocular region for recognition? In *Computer Vision and Pattern Recognition Workshops (CVPRW), 2013 IEEE Conference on*, pages 117–124. IEEE.

Tan, C.-W. and Kumar, A. (2013). Towards online iris and periocular recognition under relaxed imaging constraints. *Image Processing, IEEE Transactions on*, 22(10):3751–3765.

Tan, T., Zhang, X., Sun, Z., and Zhang, H. (2011). Noisy iris image matching by using multiple cues. *Pattern Recognition Letters*.

Vedaldi, A. and Fulkerson, B. (2010). Vlfeat: An open and portable library of computer vision algorithms. In *Proceedings of the international conference on Multimedia*, pages 1469–1472. ACM.

Woodard, D. L., Pundlik, S. J., Lyle, J. R., and Miller, P. E. (2010). Periocular region appearance cues for biometric identification. In *IEEE Computer Society Conference on Computer Vision and Pattern Recognition Workshops*, pages 162–169.

Xiong, Z., Zheng, T., Song, Z., Soong, F., and Wu, W. (2006). A tree-based kernel selection approach to efficient gaussian mixture model–universal background model based speaker identification. *Speech communication*, 48(10):1273–1282.